Optics and Lasers in Engineering 161 (2023) 107373

Contents lists available at ScienceDirect

Optics and Lasers in Engineering

journal homepage: www.elsevier.com/locate/optlaseng

Combined single/dual fiber optical trapping for flexible particle manipulation

Bingkun Gao[a], Hui Zhong[a], Bing Yan[b], LiYang Yue[b], Yuting Dang[a], Peng Chen[a], Chunlei Jiang[a,*], Zengbo Wang[b,*]

[a] College of Electrical and Information Engineering, Northeast Petroleum University, Daqing 163318, China
[b] School of Computer Science and Electronic Engineering, Bangor University, Dean Street, Bangor, Gwynedd LL57 1UT, UK

ARTICLE INFO

Keywords:
Optical trapping
Dual-fiber optical tweezers
Microparticle manipulation
Super-resolution imaging

ABSTRACT

Fiber-based optical tweezers have attracted increasing attention as a more flexible tool over conventional lens-based optical tweezers for particle manipulation. Stable trapping can be realized by single fiber gradient force, or dual fiber counter-propagating scattering forces. Both trapping modes and systems are often separately built and researched. In this paper, we demonstrate a combined single/dual fiber optical trapping (SD-FOT) system which allows dual trapping modes (i.e., single fiber gradient mode and dual fiber scattering mode) to be realized simultaneously in a single setup. Two tapered single fibers were used, with each fiber first captures a single microsphere near its tip by focus-induced gradient force; The two fibers (with trapped particles) were then aligned and adjusted to allow additional particles to be trapped and manipulated in the middle by the dual-fiber scattering trapping scheme. At least three particles will be trapped and manipulated by the combined trapping system, and each of particle can be used for *in-situ* experimental activity and analysis. Meanwhile, theoretical modeling of the optical force was established to quantify both trapping processes, and the process of the particle movement in the experiment is in accordance with the simulated force field. The developed system offers new possibilities in comparative research of single and dual fiber trapped objects and will find important applications in microsphere-based super-resolution imaging and others.

1. Introduction

Optical tweezers trapping system, firstly proposed and implemented by Ashkin [1], is a device that is capable of immobilizing and manipulating micro-objects in three dimensions using optical forces [2] in a precise and low-damage manner. It has been widely used in many fields, including force sensors [3], spectroscopy [4], optical assembly [5], especially for contributing the revolutionary advance in biological research with the advantages of single-particle and molecule trapping [6]. In 1970, Ashkin first proposed a model of radiation pressure trapping based on the scattering force to balance two back-propagating laser beams [7]. Later, Ashkin developed a gradient optical trap, a single-beam optical tweezer, which requires a single highly focused laser beam [2]. The microobject can be trapped at the position near the focus of a highly focused single beam where provides a balance of scattering and gradient forces.

The optical fiber trapping has attracted increasing attention as a more flexible tool for particle manipulation. Fiber-based optical tweezers do not require the substrate or an objective with a high numerical aperture (NA), and several fiber optical tweezers configurations have been developed for capture and movement of the dielectric and fluorescent particles [8], manipulation and separation of biological cells [9], and organization and alignment of bacteria [10]. However, the relatively short operating distance of the single-beam optical trapping system limits its operation mode and further integration with other characterization equipment. A dual-fiber trapping system could deliver a long distance of particle capture for flexible operation pairing with an objective with a large field of view [11], which leads to a wide range of applications, e.g. cell rotation based on two shear fibers [12], fiber tips based on thermal fusion stretching [13] or chemical etching [14], or tapered lens fiber tips for cell or particle manipulation [15]. In 1993, Constable et al. built one of the first fiber optic optical tweezers systems using two counter-propagating collimated single-mode fibers, which successfully captured 0.1–10 μm PS beads and active yeast cells. However, multiple capture points could be presented on the axes of the flat-ended fiber optical tweezers to cause low capture efficiency and operability [16]. In 2004, Masahiro Ikeda et al. achieved selective manipulation of symmetric plastic micro-objects using optical fiber trapping. The counterclockwise and clockwise positioning in their experiment was accomplished by the laser beams transmitted by three conical fibers with hemispherical-microsphere tips [21]. This fiber optic capture technology was widely used in biotechnology microfabrication and space technology [17]. In

* Corresponding authors.
E-mail addresses: jiangchunlei_nepu@163.com (C. Jiang), z.wang@bangor.ac.uk (Z. Wang).

https://doi.org/10.1016/j.optlaseng.2022.107373
Received 17 November 2021; Received in revised form 2 August 2022; Accepted 1 November 2022

2013, Decombe, J. B. et al. used tapered dual-fiber optical tweezers to capture one or more particles. Besides the observation by the microscope, the back signal reflected by the fibers tips gives valuable information about the trapping events [18]. In 2019, Asa Asadollahbaik et al. The use of a converging beam instead of diverging beam in dual-fiber traps creates a strong trapping efficiency in both the axial and the transverse directions. The large focal length provided by these diffractive structures allows working at a large fiber-to-fiber distance, which leads to larger space and the freedom to combine other spectroscopy and analytical methods in combination with trapping [19]. From the established literatures, it is known that the particle capture could be influenced by the divergence of the coaxially beams from a dual-fiber trapping setup, thereby affecting the observation of the captured objects.

In this paper, two single fiber trapping systems were first built, which were used to trap particle near its tip by gradient force (mode (1). These two sub-systems were then integrated as one dual-fiber optical trapping system and used to trap additional particles between the opposition fibers (mode 2). At least three particles are trapped in developed dual-mode trapping systems. By adjusting the power of the laser transmitted in the single-mode fibers, the captured middle particle can move in linear motion between two pre-captured particles. Compared to the complex and expensive optical tweezer devices of conventional devices, this low-cost optical trapping device can provide stable trapping in the working range and presents outstanding performances for realizing arbitrary hovering of the captured objects in solution. The developed system offers new possibilities in comparative research of single and dual fiber trapped objects. Meanwhile, it offers a new platform for our future research in microsphere-assisted super-resolution imaging.

2. Materials and methods

2.1. Fiber preparation and experimental principles

Fig. 1(a) shows the schematic of the experimental setup for the proposed combined Single/Dual-Fiber Optical Trapping system (SD-FOT). A diode continuous wave (CW) laser with the maximum power of 25 mW at the wavelength of 980 nm(YA605, nbyebo) is used as the light source. The laser beam is split at the ratio of 70/30 and then guided into two single-mode fibers. One of the fibers is connected to an attenuator for adjustment of the trapping force and the consequent particle movements. The tips of two optical fibers should be collimated. This process and the distance between them are precisely controlled by two individual 3D positioning stage with a step width of 50 nm. A top-view CCD camera is used to monitor the non-contact capture of the target particles through a 40x objective.

The tapered optical fiber probe is manufactured by flame heating technology [8], and the fiber tip after thermal drawing can easily capture a microsphere. (Interface type: FC/PC, core diameter: 9 μm, cladding diameter: 125 μm). In the first step, the buffer layer and polymer interlayer of the fiber are stripped using a fiber stripper to obtain a bare fiber with a diameter of 125 μm and a length of 3 cm. To improve the stability of the fibers, stainless steel capillaries are used for wrapping. The second step is to heat and draw the fiber to realize a tapered tip by an alcohol lamp. The initial drawing speed is about 5 mm/s to reduce the diameter from 125 to 10 μm for the top part with the length of 1 cm, then the drawing speed increases to about 20 mm/s to form the tapered fiber tip by the surface tension of the melted glass, as shown in Fig. 1(b). In the third step, a 3 μm diameter PS sphere is captured by the tapered fiber tip setup in solution, as shown in Fig. 1(c,d). We refer this as mode 1 trapping in the SD-FOT system, which is caused by the gradient force due to strong focus by the fiber tip. The second trapping mode, the dual-fiber scattering trapping is realized by aligning the two mode 1 fibers along the same optical axis, as shown in Fig. 1(d) Mode 2. In this case, the stable axial trapping is achieved by the balance of counter-propagating scattering forces.

2.2. Theoretical methods and calculations

The property of manipulating particles in optical traps is the combined effect of transverse and axial gradient forces playing different roles in particle manipulation [20]. In the lateral direction, the movement of the particle is caused by the gradient forces during the capture. A divergent beam with a larger capture volume can reduce the gradient forces in the lateral direction, which reduces the capture stiffness via delivery of a greater transverse moving distance for the manipulated particles [21]. Nevertheless, we used a convergent beam with the various intensity distributions instead of a normal divergent beam to cap-

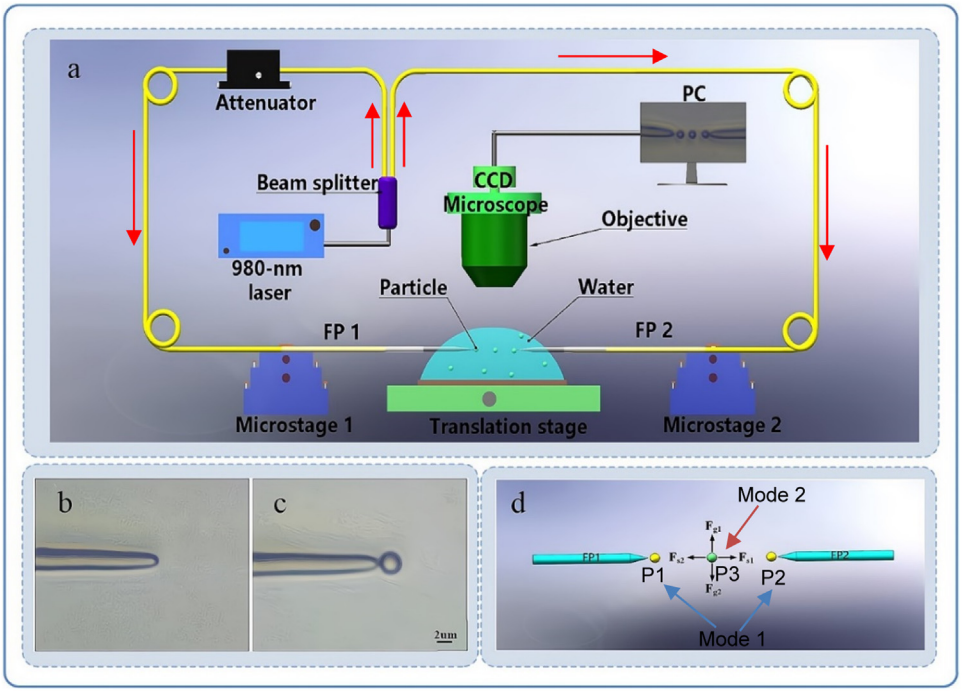

Fig. 1. (a)The experimental schematic diagram of the SD-FOT, the red arrow indicates the direction of the input laser beam. Stretch of optical fiber and capture of microspheres (b) Image of the fiber probe manufactured by heating and drawing with a parabola-like profile fiber tip. (c) Trapping of 3 μm PS spheres by single fiber gradient force. (d) Schematic diagram of dual trapping modes; Mode1: single fiber gradient trapping; Mode 2: dual fiber scattering trapping.

ture the particles in this study. The experiments demonstrated a more stable control of the particle motion than that with a diverging beam. The unbalanced axial forces led by laser power adjustment can push the particles out of the focal position; meanwhile, a strong capture effect occurs in the lateral direction due to the gradient force. Therefore, the overlap of two capture spots in the dual-fiber setup can boost the capture capability in the axial direction by balancing the output of two fibers.

The optical trapping force induced by a single laser beam is depending on the wavelength of the incident light, refractive index of the surrounding medium, and the size and refractive index of the trapped objects. For the particle whose size is much larger than the laser wavelength, the optical gradient force can be calculated by a geometric optical model through an analysis of the relationship between refractive index and conservation of momentum. For a particle with a size that is much smaller than the laser wavelength the particles are treated as point dipoles in an inhomogeneous electromagnetic field, and the gradient force can be calculated according to the Rayleigh scattering mechanism [22,23]. In addition, when the particle size is in the range of 0.1–10 λ, the light field and trapping force of the optical fiber probe should be calculated by solving Maxwell's equations. The radiation pressure force is given by [13]:

$$f + \frac{\overrightarrow{\partial g}}{\partial t} = -\nabla \cdot \vec{T} \tag{1}$$

After integration on both ends, it is expressed as:

$$\int_v f dV + \frac{d}{dt}\int_v \vec{g} dV = -\int_v \nabla \cdot \vec{T} dV = -\oint_S dS \cdot \vec{T} \tag{2}$$

Here, $\vec{g}$ is the density of the electromagnetic field in a vacuum, and $\vec{T}$ is the Maxwell stress tensor which can be expressed as:

$$T_{ik} = \frac{\varepsilon_0\varepsilon_1\left|\vec{E}\right|^2 + \mu\mu_0\left|\vec{H}\right|^2}{2}\delta_{ik} - \varepsilon_0\varepsilon_1 E_i E_k - \mu\mu_0 H_i H_k \tag{3}$$

Here, $\vec{E}$ *and* $\vec{H}$ are the vectors of electromagnetic fields in free space; under the label, k represents x, y or z dimensions; ε_0, and ε_1 respectively represent the dielectric constant of the vacuum and the medium; μ, μ_0 are magnetic permeability in media and vacuum, respectively. For TM mode beam propagating along z-axis with non-zero electromagnetic field components (H_y, E_x, E_z), the, the radiation pressure of a particle on the x and z axes can be calculated as:

$$F_z = \frac{1}{2}\oint_s \left[-\frac{1}{2}\left(\mu\mu_0\left|H_y\right|^2 + \varepsilon_0\varepsilon_1\left|E_x\right|^2 - \varepsilon_0\varepsilon_1\left|E_z\right|^2\right)dx + \varepsilon_0\varepsilon_1 Re\left(E_x E_z^*\right)dz\right] \tag{4}$$

$$F_x = \frac{1}{2}\oint_s \left[-\frac{1}{2}\left(\mu\mu_0\left|H_y\right|^2 + \varepsilon_0\varepsilon_1\left|E_z\right|^2 - \varepsilon_0\varepsilon_1\left|E_x\right|^2\right)dz + \varepsilon_0\varepsilon_1 Re\left(E_z E_x^*\right)dx\right] \tag{5}$$

Similarly for TE mode (E_x, H_y, H_z), the force can be calculated as:

$$F_y = \frac{1}{2}\oint_s \left[\frac{1}{2}\left(\mu\mu_0\left|H_y\right|^2 - \varepsilon_0\varepsilon_1\left|E_x\right|^2 - \mu\mu_0\left|H_z\right|^2\right)dz + \mu\mu_0 \mathrm{Re}\left(H_y H_z^*\right)dy\right] \tag{6}$$

$$F_z = \frac{1}{2}\oint_s \left[\frac{1}{2}\left(\mu\mu_0\left|H_z\right|^2 - \varepsilon_0\varepsilon_1\left|E_x\right|^2 - \mu\mu_0\left|H_y\right|^2\right)dy + \mu\mu_0 \mathrm{Re}\left(H_z H_y^*\right)dz\right] \tag{7}$$

Here S is the contour line of the particle enclosed in the XOZ and YOZ planes, for TM and TE polarization, respectively. By integrating the x, y, or z component of forces (FO) over the distance D from the origin of the coordinate, the trapping potential U can be obtained along different directions:

$$U = -\int F_o dD \tag{8}$$

For 3D particles, the final force is calculated as combination of forces on all enclosing faces surrounding the particles. In this work, the 3D electromagnetic field distribution of SD-FOT system was firstly calculated using a commercial software CST Microwave Studio, with microsphere presented in different locations and configurations. The force was then calculated using a post-processing MATLAB code based on above formulations.

3. Results

3.1. Theory of optical fields and forces

Fig. 2 shows simulated optical fields and forces which explain the physics of the dual operation modes in the SD-FOT system. From Fig. 2a we can see our tapered fiber tip generates a strong near-field focusing. When a 3 μm PS particle was brought close to the fiber, it interacts with the tip focusing and affects the overall field distribution (see Fig. 2b). The corresponding axial trapping force, as shown in Fig. 2d, reveals that the 3 μm PS particle can be stably trapped at axial position close to the tip, and particle experiences pull forces when distance from the tip is less than 4 μm. The equilibrium position is about 200 nm away from the fiber tip. This explains the single fiber trapping mode (mode 1) in our setup. Then, when an additional 1 μm PS particle was brought close to the stably trapped 3 μm PS particle, the near-field pattern further changed (see Fig. 2c). Here, the calculated axial trapping force for the 1 μm PS particle doesn't shown any pull force toward the larger 3 μm particle, but only push force caused by forward scattering (see Fig. 2e). Therefore, the particles are subjected to gradient forces only in the lateral direction, which can be achieved by adjusting the laser power to oscillate back and forth. To balance this force for stable trapping, we need bring in second fiber tip with same design thus a dual-fiber configuration. Note we haven't conducted dual fiber analysis where coherent beam interference effect may affect the theorical trapping efficiencies. However, our current single fiber-based theory can successfully explain the dual-trapping modes. Beside axial trapping cases, we also calculated transverse trapping force and potential for the 1 μm PS particle (Fig. 2c case). The results shown in Fig. 2(f,g) reveal the stable transverse trapping can be easily obtained and maintained in our dual-mode trapping system, with maximum lateral trapping force and potential being reached at the center of the beams.

3.2. Experimental demonstration of SD-FOT dual-mode trapping

Fig. 3 demonstrates the simultaneous dual-mode trapping of PS microspheres. A total of three particles were involved. Each fiber tip capturers a 3 μm PS particle (mode 1: single fiber trapping) and then used for dual-fiber trapping of 1 μm between them. The two fibers are fixed on an adjustable three-dimensional table. The distance between two collimated fiber probes is 6–20 μm, and the laser power is tuned to 18 mW for carrying out the linear motion experiment. At the beginning, the middle PS particle is still on the optical axis because of the balanced transverse gradient force and the canceled repulsive scattering force. The moving process of the captured particle from left to right is shown in Fig. 3(a–e) with time, power increase from 0 mW to 3 mW.At $t = 2.5$ s, the captured particle reached the position of the right microsphere while increasing the laser power from left fiber. As shown in Fig. 3(f–i), when the laser power outputted from 3 mW to 8 mW.The right-hand fiber is larger, the particle can move back to the left fiber probe again. When two optical fibers are assembled into a microsphere lens by capturing two microspheres separately through a gradient force, the microsphere lenses are closer together when their focal points coincide at the same position, which makes the particles stay stably at the position of the focal point.

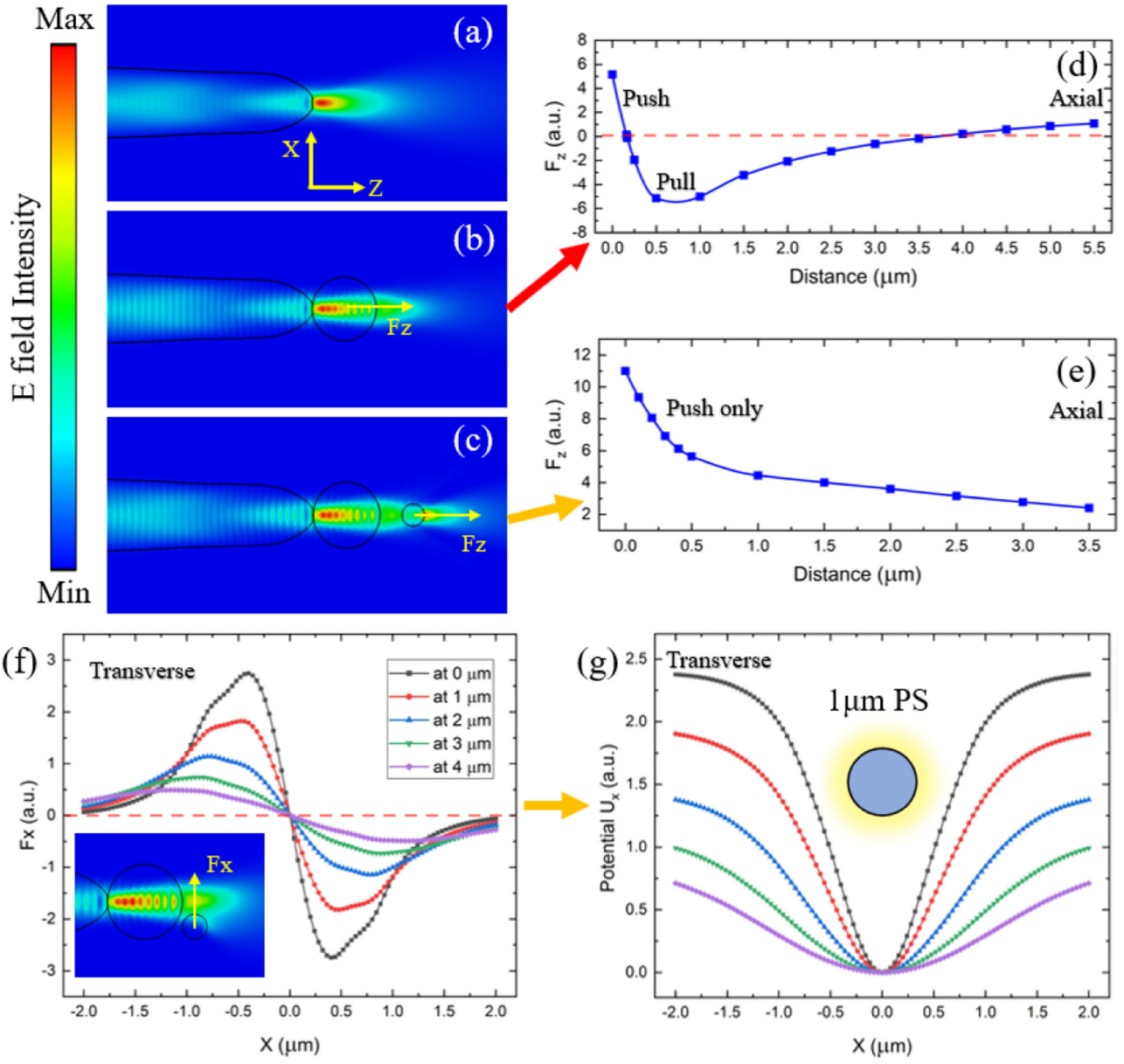

Fig. 2. Calculated optical fields and forces showing two different trapping mechanisms in the SD-FOT system. (a, b, c) electric intensity field |E|2 distribution for the bare fiber tip, with 3 μm PS particle, and with 3 μm and 1 μm PS particles, respectively. (d) Axial force as a function of distance from the tip of the fiber for case (b), showing 3 μm PS can be stably trapped. (e) axial force for 1 μm PS particle, showing the particle experiences push force only. (f,g) transverse gradient force and corresponding trapping potential for the 1 μm PS particle.

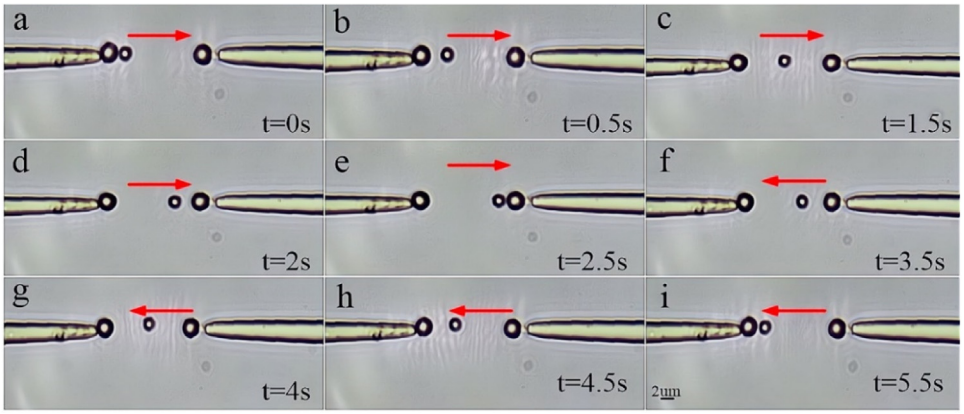

Fig. 3. Experimental optical microscope image of dual-mode trapping and the transfer process, the red arrows represent the direction of transport of the particles. (a) The tapered tip captures the particles, ready to control and manipulate the intermediate PS particles under the condition that the two fibers are axially aligned. (b–e) Increasing the laser power of the left fiber, the particle is moved towards the right fiber by the force. (f–i) Increasing the laser power of the right fiber moves the particle towards the left fiber under the force of the laser.

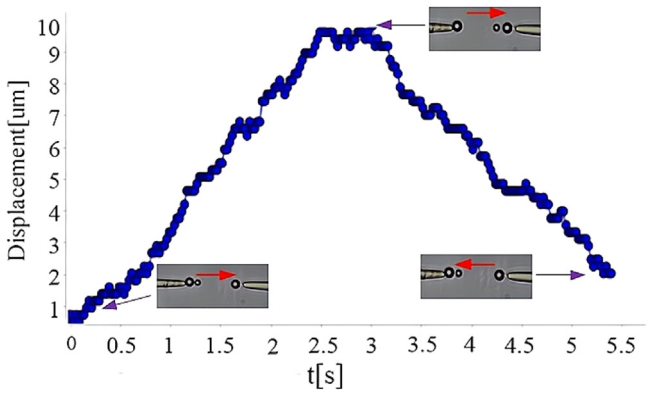

Fig. 4. Position tracking of particle motion as in Fig. 3.

In the experiment, we find the pattern of particle size by varying the size of the captured particles and the size of the manipulated particles. First, two optical fibers were used to capture 3 μm PS particles to manipulate 1 μm and 2 μm particles, respectively, and the manipulation of particles could be achieved under arbitrary power body adjustment. When the captured PS particles are greater than or equal to 3 μm, the position of the particles will not change when the particles move close to the tip of the fiber, and it is impossible to explore the imaging characteristics of microsphere-based super-resolution imaging by adjusting the laser power. Therefore, the experimental purpose can be achieved only when the diameter of the first captured particle is larger than that of the second captured particle. In this process, we employ two tapered single fibers, each of which first captures a microsphere near its tip by focus-induced gradient forces, between the two fibers to capture and manipulate and a third particle. And comparing with the two fibers manipulating particles without capturing microspheres, it can be found that the former manipulates particles to stay in a certain position more stably.

Fig. 4 shows the tracked position of the middle particle motion as in Fig. 3. The movement generally follows a linear relationship which can be used to estimate the particle velocity (reciprocal of the slope). Some local variation occurs due to the fluctuation of suspension and laser scattering, but the trapping remains always stable. The develop SD-FOT system thus offers robust performance in trapping and driving of the microsphere objects. In our experiments, the middle microsphere becomes detached from the light trap due to Brownian motion and the microspheres cannot be controlled, it is found when the distance between the dual fiber reaches about 40 μm and more.

4. Discussion

In this article, the demonstrated SD-FOT system supports two trapping modes simultaneously, i.e., single-fiber gradient trapping and dual-fiber counter-facing trapping in a single system. Two tapered single fibers were used, with each fiber first captures a single microsphere near its tip by focus-induced gradient force; The two fibers (with trapped particles) were then aligned and adjusted to allow additional particles to be trapped and manipulated in the middle by the dual-fiber scattering trapping scheme. The converging beam produced by a single fiber (with trapped particles) will only capture additional particles in the lateral direction, and each of particle can be used for *in-situ* experimental activity and analysis. The use of optical fibers with microspheres is more stable when manipulating additional particles. Support is provided for the development of a flexible micromanipulation technique for scanning microsphere super-resolution imaging applications. For example, we can keep two fiber-trapped particles static, and then introduce different sizes of microsphere in between to scan along the optical axis. In this case, super-resolution imaging performance between static and scanning imaging modes, as well as by different-sized microspheres, can be studied inside solution in real time. The scanning speed can be controlled by tunning the laser powers. This will greatly speed up the development of more advanced microsphere super-resolution imaging system for studying biological samples. Non-invasive super-resolution imaging can be achieved by properly developing the imaging properties of the microsphere superlens explored in this study. More particles could be introduced within the optical axis which will provide even more efficient parallel imaging capabilities. Therefore, the proposed method has the potential to non-invasively realize live-cell structural information acquisition and specific molecule tracking concurrently, which facilitates studying rare subcellular events in their cellular environment and over a complete life period.

5. Conclusion

In this paper, a dual trapping mode optical fiber trapping system SD-FOT has been demonstrated for effective capturing and manipulation of multiple particles in water. Its feasibility was tested through the capture of three PS particles of different sizes in this study. The linear motion of the particle between two fiber-trapped microspheres can be controlled by the laser output power, and the corresponding setup is simpler than that for the conventional optical tweezers. The SD-FOT will contribute to the development of next-generation microsphere-based super-resolution imaging technique and others.

Funding

This work was supported by the Joint Guidance Project of Natural Science Foundation of Heilongjiang Province, China (No. LH2021F008).

Declaration of Competing Interest

The authors declare no conflict of interest.

Data Availability

No data was used for the research described in the article.

References

[1] Ashkin A. Acceleration and trapping of particles by radiation pressure. Phys Rev Lett 1970;24:156–9.
[2] Ashkin A, Dziedzic JM, Bjorkholm JE, Chu S. Observation of a single-beam gradient force optical trap for dielectric particles. Opt Lett 1986;11:288–90.
[3] Marago OM, Jones PH, Bonaccorso F, Scardaci V, Gucciardi PG, Rozhin AG, Ferrari AC. Femtonewton force sensing with optically trapped nanotubes. Nano Lett 2008;8:3211–16.
[4] Wang F, Toe WJ, Lee WM, McGloin D, Gao Q, Tan HH, Jagadish C, Reece PJ. Resolving Stable Axial Trapping Points of Nanowires in an Optical Tweezers Using Photoluminescence Mapping. Nano Lett 2013;13:1185–91.
[5] Gargiulo J, Violi IL, Cerrota S, Chvatal L, Cortes E, Perassi EM, Diaz F, Zemanek P, Stefani FD. Accuracy and mechanistic details of optical printing of single Au and Ag nanoparticles. ACS Nano 2017;11:9678–88.
[6] Abbondanzieri EA, Greenleaf WJ, Shaevitz JW, Landick R, Block SM. Direct observation of base-pair stepping by RNA polymerase. Nature 2005;438:460–5.
[7] Ashkin A. Acceleration and trapping of particles by radiation pressure. Phys Rev Lett 1970;24:156 -&.
[8] Xin HB, Xu R, Li BJ. Optical trapping, driving, and arrangement of particles using a tapered fibre probe. Sci Rep 2012;2:8.
[9] Li YC, Xin HB, Cheng C, Zhang Y, Li BJ. Optical separation and controllable delivery of cells from particle and cell mixture. Nanophotonics 2015;4:353–60.
[10] Liu XS, Huang JB, Zhang Y, Li BJ. Optical regulation of cell chain. Sci Rep 2015;5:11.
[11] van der Horst A, van Oostrum PD, Moroz A, van Blaaderen A, Dogterom M. High trapping forces for high-refractive index particles trapped in dynamic arrays of counterpropagating optical tweezers. Appl Opt 2008;47:3196–202.
[12] Black BJ, Mohanty SK. Fiber-optic spanner. Opt Lett 2012;37:5030–2.
[13] Liu ZH, Guo CK, Yang J, Yuan LB. Tapered fiber optical tweezers for microscopic particle trapping: fabrication and application. Opt Express 2006;14:12510–16.
[14] Liu ZL, Liu YX, Tang Y, Zhang N, Wu FP, Zhang B. Fabrication and application of a non-contact double-tapered optical fiber tweezers. Opt Express 2017;25:22480–9.
[15] Lyons ER, Sonek GJ. Demonstration and modeling of a tapered-lensed optical fiber trap, micro-optics/micromechanics and laser scanning and shaping. Int Soc Opt Photonics 1995;2383:186–98.

[16] Constable A, Kim J, Mervis J, Zarinetchi F, Prentiss M. Demonstration of a fiber-optical light-force trap. Opt Lett 1993;18:1867–9.
[17] Ikeda M, Tanaka K, Kittaka M, Tanaka M, Shohata TA. Rotational manipulation of a symmetrical plastic micro-object using fiber optic trapping. Opt Commun 2004;239:103–8.
[18] Decombe JB, Huant S, Fick J. Single and dual fiber nano-tip optical tweezers: trapping and analysis. Opt Express 2013;21:30521–31.
[19] Asadollahbaik A, Thiele S, Weber K, Kumar A, Drozella J, Sterl F, Herkommer AM, Giessen H, Fick J. Highly efficient dual-fiber optical trapping with 3D printed diffractive fresnel lenses. ACS Photonics 2019;7:88–97.
[20] Asadollahbaik A, Thiele S, Weber K, Kumar A, Drozella J, Sterl F, Herkommer AM, Giessen H, Fick J. Highly efficient dual-fiber optical trapping with 3D printed diffractive fresnel lenses. ACS Photonics 2020;7:88–97.
[21] Zhang Y, Liang P, Liu Z, Lei J, Yang J, Yuan L. A novel temperature sensor based on optical trapping technology. J Light Technol 2014;32:1394–8.
[22] Bradac Carlo. Nanoscale optical trapping: a review. Adv Opt Mater 2018;6:1800005.
[23] Kotlyar VV, Nalimov AG. Analytical expression for radiation forces on a dielectric cylinder illuminated by a cylindrical Gaussian beam. Opt Express 2006;14:6316–21.